J. Inst. Eng. India Ser. E (December 2023) 104(2):223–235
https://doi.org/10.1007/s40034-023-00280-w

ORIGINAL CONTRIBUTION

Intimation of Gravitational Body Forces in Magnetized Transport of Bio-Nanofluid Flow with Bioconvection and Variable Viscosity

Muhammad Jawad[1,2] · **Muhammad Sajid**[3]

Received: 9 December 2022 / Accepted: 23 November 2023 / Published online: 10 December 2023

Abstract On account of technological and industrial applications, nanofluids are more realistic to boost heat transfer as compared to simple fluids. Therefore, the contemporary mathematical study offers a theoretical analysis regarding incompressible, time-independent electrical magnetohydrodynamic nanofluid flow over a vertical stretching surface. In addition, the influence of convective boundary conditions along with gravitational body forces is considered. To explore the performance of the nanofluid with a viscosity variable for different bodily impacts, we deliberated Brownian motion and thermophoresis parameters in the flow. A well-known shooting technique was implemented to numerically solve the nonlinear system of governing equations. Throughout, the significance of emerging parameters like bioconvection parameter, Peclet number thermophoresis, Lewis numbers, Brownian motion, Prandtl number, magnetic parameter and Schmidt number is elucidated via plots, whereas the division of numerous appreciated physical measures like local Nusselt number, coefficient of skin friction, local Sherwood number and local density of the motile microorganisms is also tabulated. The core finding of the current study is that it helps to control the rate at which heat is transported as well as fluid speed in any industrial applications to make wanted nature of the eventual outcome.

✉ Muhammad Jawad
jawadsial37@gmail.com

[1] Faculty of Sciences, The Superior University, Lahore, Pakistan

[2] Department of Mathematics, The University of Faisalabad, Faisalabad, Pakistan

[3] Institute of Microscale Optoelectronics, Optical Engineering, Shenzhen university, Shenzhen, China

Keywords Gravitational body forces · Swimming microorganism · Variable viscosity · Magnetohydrodynamics · Stretching sheet

Abbreviations

BVP	Boundary value problem
IVP	Initial value problem
MHD	Magnetohydrodynamics
ODEs	Ordinary differential equations
PDEs	Partial differential equation

List of symbols

M	Harman number
λ	Variable viscosity
Pr	Prandtl number
R_{ex}	Local Reynolds number
δ	Swimming microorganism intensity variation parameter
Nt	Thermophoresis parameter
Lb	Bioconvection Lewis number
B_T	Local concentration Grashof number
Nb	Brownian motion parameter
Sc	Schmidt number
Gr	Thermal Grashof numbers
Br	Concentration Grashof numbers
Pe	Peclet number
G_T	Local thermal Grashof number
(u, v)	Components of velocity

Introduction

In recent days, the development of the computer age, communication, household appliances, heavy mechanical industries, transportation and the electronics industries have all been running due to some electronics and mechanical devices. To prevent overheating all these devices, a system of cooling or heating is built in which fluid flows over or around the device at a certain temperature threshold.

The improvement in the thermal conductivity of conventional fluids is imperative because many mechanical and electronic devices have retarded their efficiency and working age, as conventional fluids with low thermal conductivity do not occur at the temperature essential. Non-Newtonian fluids have the devotion of engineers and scientists due to their vast applications in the fields of manufacturing, technology and energy. Regular examples of such fluids are fiber technology, rubber sheet manufacturing, plastic, wall paint, polymer processes, lubricants, enhanced oil recovery, plastic, shampoo, greases, blood, mud, food production, toothpaste, ketchup, and drilling. Nanofluid is one of the most important types of non-Newtonian fluids. Nanofluids are the suspension of nanomaterial's (e.g., nanoparticles, nanosheets, nanofibers, nanotubes, nanowires, nanorods, or droplets) in base fluids.

In the modern era, nanofluids are the center of attention for many researchers due to their wide range of applications. Suspension of nanoparticles in conventional fluids is termed nanofluids, where nanoparticles include metallic and nonmetallic particles of nanosize. For the very first time, Choi [1] introduced the concept of nanofluids. A thin suspension of nanoparticles and base fluids makes nanofluids. Buongiorno [2] developed the numerical study of nanofluids that measure Brownian motion as well as thermophoresis features. Khan and Pop [3] presented a numerical study for nanofluid flow with effects of thermophoresis and Brownian motion via a linearly extending plate. Tiwari and Das [4] studied the mathematical model, which is very important to observe a strong volume fraction of nanomaterials in the regular fluid. Arifin et al. [5] inspected the dynamics of flow suction as well as joule heating and the thermal features of the hybrid (copper and aluminum oxide) nanofluid due to the parallel shrinking and stretching of the film with the combined influence of electrical conducting fluids. Shafiq et al. [6] discussed the flow properties of third-class non-Newtonian nanoliquid over a vertically extending disk. Micro-polar hybrid nanofluid with the impact of slip conditions across the Riga channel has been scrutinized by [7].

An analysis of bioconvection for nanofluid flow in an acoustically dominated source has been investigated by Mansour et al. [8]. Kolsi et al. [9] deliberated the utilization of nanoliquid on a cuboidal surface in occurrence of magnetic flux. The effect of flow rate and buoyancy force with such mass flow features over Sisko nanofluid owing to stretched surfaces in the presence of porous channels has been discovered by Sharma et al. [10].

Due to the various applications of fluid flow over stretching sheets in metallurgy and plastic engineering, it has become a center of research. Crane [11] was the first to deliberate the momentum boundary layer of a linearly extending sheet. Later on, many investigators studied and explored the idea of a stretching sheet [12–21]. Recently, [22] analyzed the influence of variable viscosity and second-order slip flow on hybrid nanofluids over the porous extending sheet.

The study of magnetohydrodynamics MHD flow plays various roles in different industrial and engineering applications. In industrial applications, the most important roles are liquid metal fluid, metal turning, glass blowing, aerodynamics, and cooling in nuclear plants. In engineering applications used in metal spinning and polymer extrusion, drawing plastic film, paper production and producing cooling when a product is manufacturing. The electrical conducting flow of nanofluids, along with thermophoresis by HAM is studied by [23]. Hayat et al. [24], with the assistance of HAM, inspected the electrical MHD flow of nanofluids due to an extending plate along with buoyancy forces in the occurrence of a magnetic field. Khan et al. [25] examined the magnetohydrodynamics of incompressible flow through a rotating disk using coupled stress fluid. Hayat et al. [26] discovered the magnetohydrodynamic (MHD) consequences of squeezing flow in Jeffery nanofluid.

By witness of above survey of literature current analysis are not preform yet, our attention is to evaluate the magnetohydrodynamic MHD magnetized transport of nanofluid flow with the swimming of gyrotactic microorganisms and variable viscosity due to vertical stretching sheet. The influence of convective boundary conditions along with gravitational body forces is also a segment of this study. The literature survey reveals that such analyses have not been performed yet. The consideration of non-Newtonian viscous nanofluids, swimming motile microorganisms, and the impact of variable viscosity made this analysis quite motivating. The associated boundary value problem is solved numerically by using the shooting technique after converting it into a first-order initial value problem. The physical features of effective parameters are graphically underlined and discussed for involved profiles.

Mathematical Analysis

A steady MHD transport of nanofluid toward a stretching sheet with variable viscosity and convective boundary conditions has been under consideration. The theory of microorganisms is used through bioconvection to alleviate the suspended nanoparticles under the influence of buoyancy forces where it is taken as a coordinate system. A magnetic

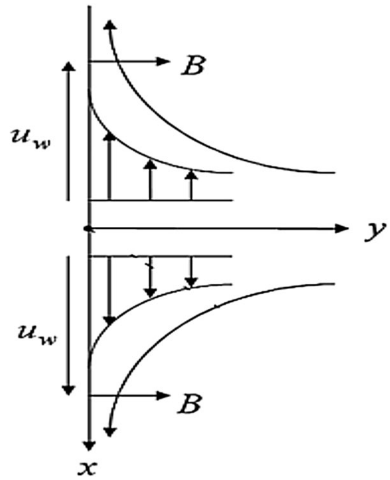

Fig. 1 Geometry of problem

field of strength is induced in the fluid, and it is assumed that the sheet is stretching along the x-direction. In the presence of gravitational body forces, the corresponding governing equations for nanofluid can be described as [27–31] (see Fig. 1).

The equation of Mass Conservation

$$\frac{\partial u}{\partial x}+\frac{\partial v}{\partial y}=0 \tag{1}$$

Equation of Velocity

$$\rho\left(u\frac{\partial u}{\partial x}+v\frac{\partial u}{\partial y}\right)=\frac{\partial}{\partial y}\left[\mu(T)\left(\frac{\partial u}{\partial y}\right)\right]-\sigma B_0^2u+g\rho B_T\left(T-T_\infty\right)+\rho gB_C\left(C-C_\infty\right) \tag{2}$$

Equation of Temperature

$$\rho c_P\left(u\frac{\partial T}{\partial x}+v\frac{\partial T}{\partial y}\right)=\alpha\left(\frac{\partial^2 T}{\partial y^2}\right)+\tau\left\{\frac{D_T}{T_\infty}\left(\frac{\partial T}{\partial y}\right)^2+D_B\frac{\partial C}{\partial y}\frac{\partial T}{\partial y}\right\} \tag{3}$$

Equation of Concentration

$$u\frac{\partial C}{\partial x}+v\frac{\partial C}{\partial y}=D_B\frac{\partial^2 C}{\partial y^2}+\frac{D_T}{T_\infty}\frac{\partial^2 T}{\partial y^2} \tag{4}$$

Equation of Density of Microorganism

$$u\frac{\partial N}{\partial x}+v\frac{\partial N}{\partial y}+\left[\frac{bW_c}{C_W-C_\infty}\right]\left(\frac{\partial N}{\partial y}\frac{\partial C}{\partial y}+N\frac{\partial^2 C}{\partial y^2}\right)=D_n\frac{\partial^2 N}{\partial y^2} \tag{5}$$

where u and v are velocity constituents along $x-axis$ and $y-axis$, respectively, and B_0 represents the strength magnetic field, while N, T, and C are density, energy, and concentration of nanofluid, respectively. Equations (2)–(5) are subjected to:

for $y=0, u=u_w(x)=bx, v=0,$

$$k_f\frac{\partial T}{\partial y}h_f\left(T-T_f\right),\ C=C_w\ and\ T=T_w \tag{6}$$

$$as\ y\to\infty,\ u,v\to 0,\ T\to T_\infty,\ C\to C_\infty\ and\ N\to N_\infty \tag{7}$$

The similarity transformation and dimensionless variables are described as

$$\psi=(bv)^{\frac{1}{2}}xf(\eta),\ u=bxf'(\eta),\ and\ \eta=\left(\frac{a}{v}\right)^{\frac{1}{2}}y,\ v=\sqrt{bv}f(\eta),\ and \tag{8}$$

$$\left(T_w-T_\infty\right)\theta(\eta)=T-T_\infty,\ \left(C_w-C_\infty\right)\phi(\eta)=C-C_\infty,\ \left(N_w-N_\infty\right)\chi(\eta)=N-N_\infty, \tag{9}$$

where ψ is the stream function and η is the similarity variable defined as $u=\frac{\partial\psi}{\partial y}$ and $v=-\frac{\partial\psi}{\partial x}$, which directly satisfies the equation of mass conservation. The viscosity of fluid in momentum equation is temperature-dependent that may vary exponentially [35].

$$\mu(T)=\mu_0e^{-H(T-T_\infty)} \tag{10}$$

where μ_0 represents the fluid viscosity at T_∞. The strength dependency between $\mu(T)$ and T are depicted by H. Utilizing the similarity variables illustrated in Eqs. (8 and 9) and then applying the Maclaurin's expansion, we obtained the succeeding illustration [32]

$$e^{-\lambda\theta}=1-\lambda\theta+O\left(\lambda^2\right) \tag{11}$$

Now, by using the similarity function given in Eqs. (8–9), the subsequent dimensionless coupled equations has been accomplished

$$(1-(\lambda\theta))f'''(\eta)-\lambda\theta'(\eta)f''(\eta)+f(\eta)f''(\eta)-f'^2-Mf'(\eta)+G_r\theta(\eta)+B_r\theta(\eta)=0 \tag{12}$$

$$\theta''(\eta)+Prf(\eta)\theta'(\eta)+Pr(Nb)\theta'(\eta)\phi'(\eta)+Pr(Nt)\theta'^2(\eta)=0 \tag{13}$$

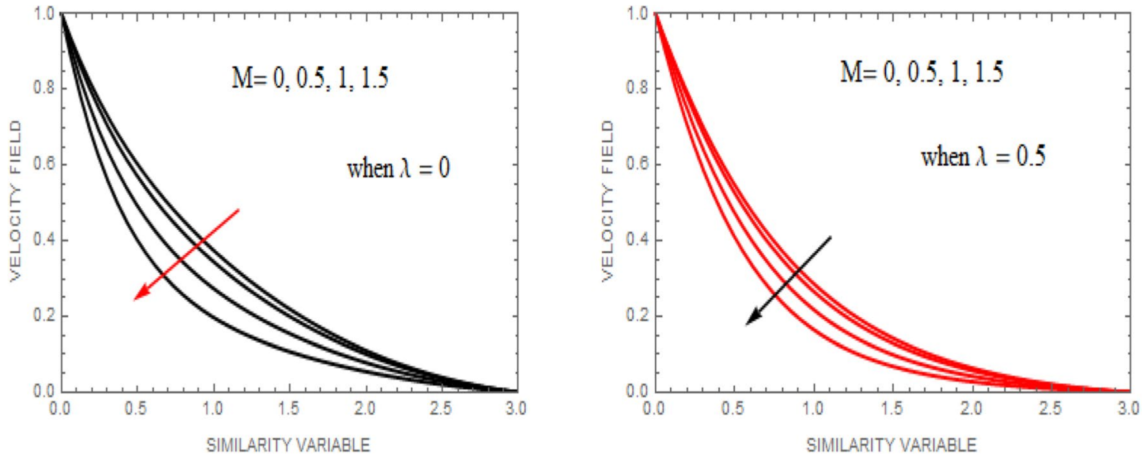

(a) Effects of Harman number M over $f'(\eta)$ when $\lambda = 0$

(b) Effects of Harman number M over $f'(\eta)$ when $\lambda = 0.5$

Fig. 2 Effects of Harman number M over $f'(\eta)$

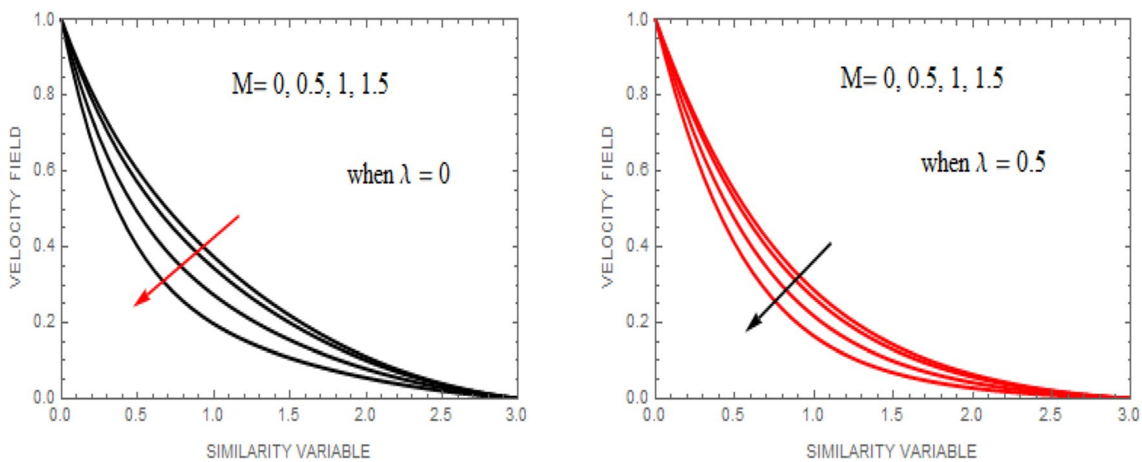

(a) Effects of Harman number M over $\theta(\eta)$ when $\lambda = 0$

(b) Effects of Harman number M over $\theta(\eta)$ when $\lambda = 0.5$

Fig. 3 Effects of Harman number M over $\theta(\eta)$

$$\phi''^{(\eta)} + Scf(\eta)\phi'^{(\eta)} + \left(\frac{Nt}{Nb}\right)\theta''(\eta) = 0 \tag{14}$$

$$\chi''(\eta) + Lbf(\eta)\chi'(\eta) - Pe\left(\phi''(\chi + \delta) + \chi'(\eta)\phi'(\eta)\right) \tag{15}$$

where $M = \frac{B^2{}_0\sigma}{b\rho}$ is Harman number, $\lambda = H(T_w - T_\infty)$ is the variable viscosity, $Pr = \frac{\upsilon}{\alpha}$ is the Prandal number, $R_{ex} = \frac{u_w(x)x}{\upsilon}$ is local Reynoled number, $\delta = \frac{N_\infty}{N_w - N_\infty}$ is swimming microorganism intensity variation parameter, $Nt = \frac{\tau\rho D_T(T_w - T_\infty)}{\mu_0 T_\infty}$ is thermophoresis parameter, $Lb = \frac{\upsilon}{D_n}$ is bioconvection lewis number, $B_T = \frac{g\rho B_T(C_w - C_\infty)X^3}{\upsilon^2}$ is local concentration Grashof number, $Nb = \frac{\tau\rho D_B(C_w - C_\infty)}{\mu_0}$ is Brownian motion parameter, $Sc = PrLe$ is Schmidt number, $Gr = \frac{G_T}{R^2{}_{ex}}$ and $Br = \frac{B_T}{R^2{}_{ex}}$ are concentration and thermal Grashof numbers, $Pe = \frac{bWc}{D_n}$ is Peclet number, and $G_T = \frac{g\rho B_T(T_w - T_\infty)X^3}{\upsilon^2}$ is local thermal Grashof number.

The auxiliary conditions in dimensionless form are:

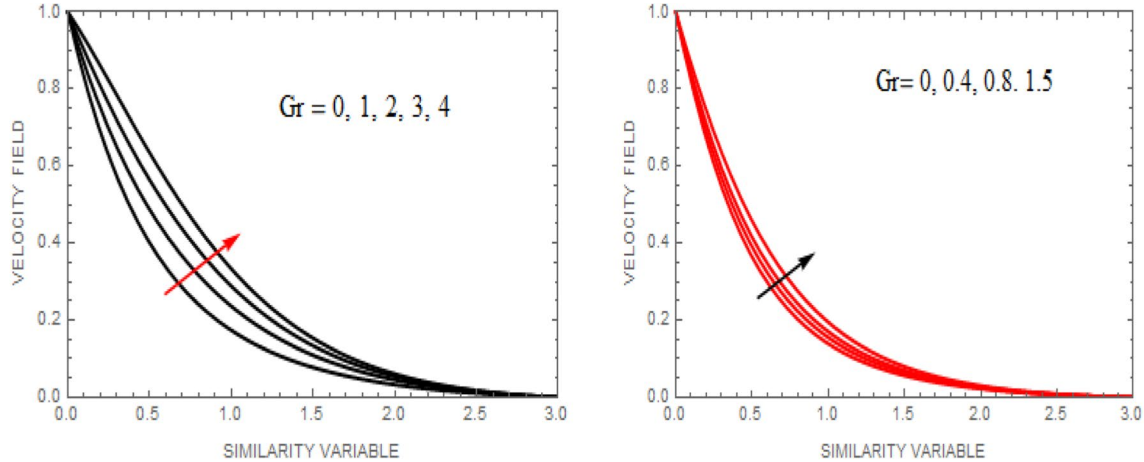

(a) Effects of thermal Grashof number Gr over $f'(\eta)$ when $\lambda = 0$

(b) Effects of thermal Grashof number Gr over $f'(\eta)$ when $\lambda = 0.5$

Fig. 4 Effects of thermal Grashof number Gr over $f'(\eta)$

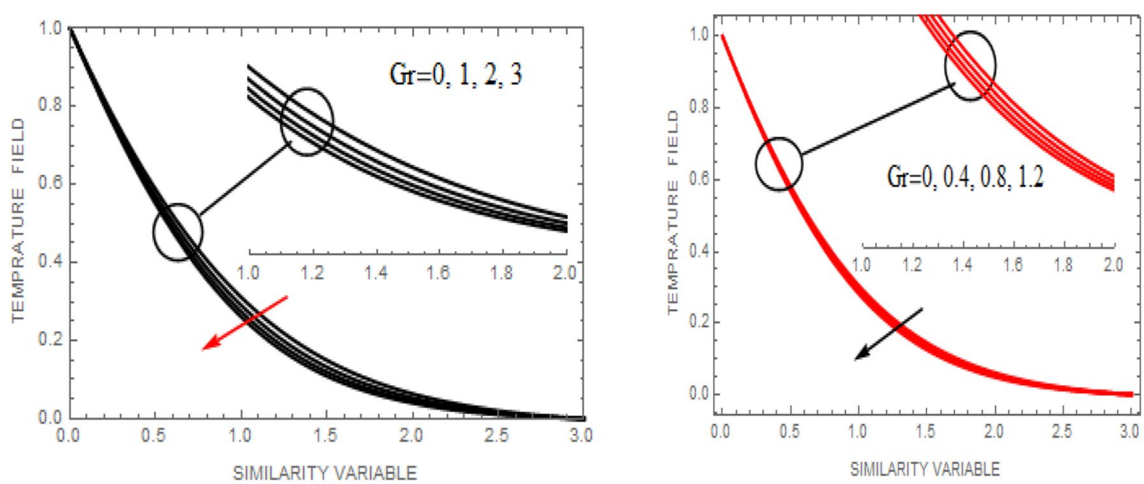

(a) Effects of thermal Grashof number Gr over $\theta(\eta)$ when $\lambda = 0$

(b) Effects of thermal Grashof number Gr over $\theta(\eta)$ when $\lambda = 0.5$

Fig. 5 Effects of thermal Grashof number Gr over $\theta(\eta)$

$$At\ \eta = 0,\ f(\eta) = 0,\ \chi(\eta) = 1,\ \theta'(\eta) = -B_i(1 - \theta(\eta)),\ f'(\eta) = 0,\ \phi(\eta) = 1 \tag{16}$$

$$as\ y \to \infty,\ \phi(\eta) = \chi(\eta) = \theta(\eta) = 0,\ f'(\eta) = 0 \tag{17}$$

Physical quintiles of interest, like microorganism density number, local Sherwood number, local Nusselt number, and skin fraction coefficient, are defined as:

$$C_f = \frac{\tau_w}{\rho U_w^2},\ Nu_x = \frac{xq_w}{k(T_w - T_\infty)},\ Sh_x = \frac{xq_m}{D_B(C_w - C_\infty)},\ Nn_x = \frac{xq_m}{D_n(N_w - N_\infty)} \tag{18}$$

where

$$\tau_w = \mu\left(\frac{\partial u}{\partial y}\right)_{y=0},\ q_w = -k\left(\frac{\partial T}{\partial y}\right)_{y=0},\ q_m = D_B\left(\frac{\partial C}{\partial y}\right)_{y=0},\ q_n = -D_n\left(\frac{\partial N}{\partial y}\right)_{y=0} \tag{19}$$

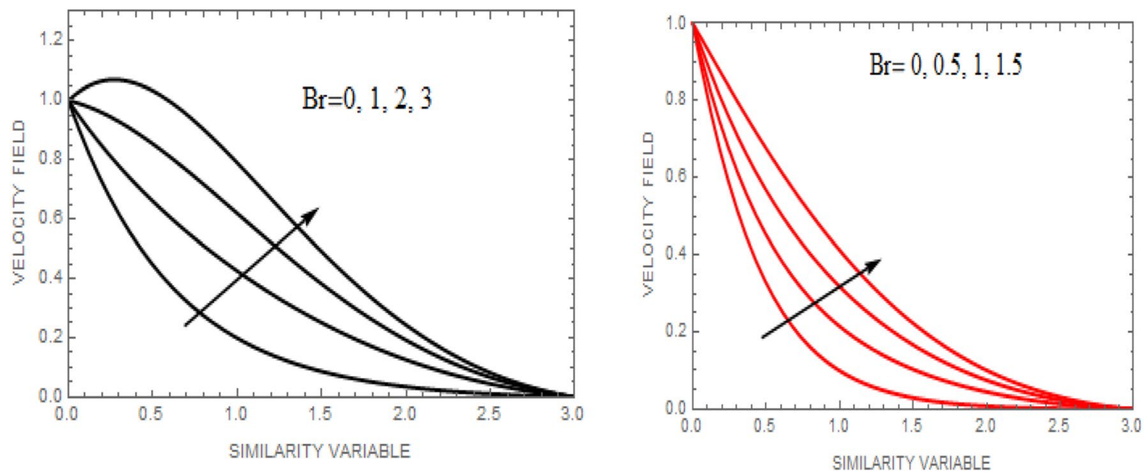

(a) Effects of concentration Grashof number Br over $f'(\eta)$ when $\lambda = 0$

(b) Effects of concentration Grashof number Br over $f'(\eta)$ when $\lambda = 0.5$

Fig. 6 Effects of concentration Grashof number Br over $f'(\eta)$

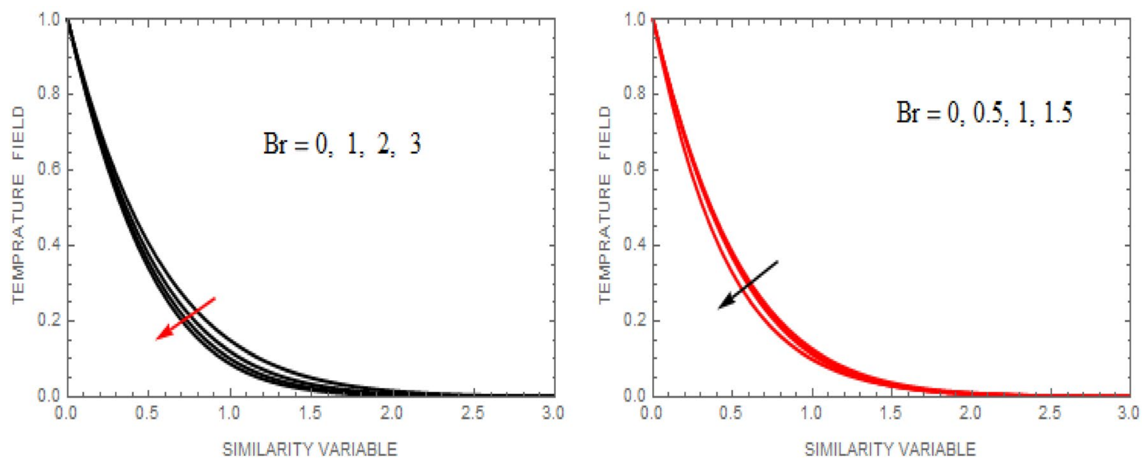

(a) Effects of concentration Grashof number Br over $\theta(\eta)$ when $\lambda = 0$

(b) Effects of concentration Grashof number Br over $\theta(\eta)$ when $\lambda = 0.5$

Fig. 7 Effects of concentration Grashof number Br over $\theta(\eta)$

So dimensionless form becomes as

$$C_f \mathrm{Re}_x^{1/2} = (1 - \lambda\theta(0))f''(0),\ Nu_x \mathrm{Re}_x^{-1/2} = -\theta'(0),$$
$$Sh_x \mathrm{Re}_x^{-1/2} = -\phi'(0),\ Nn_x \mathrm{Re}_x^{-1/2} = -\chi'(0) \tag{20}$$

Numerical Technique

In daily life, many mathematical models of equations are highly nonlinear differential equations. We know that exact solutions to extremely nonlinear differential equations are not usually possible. In cases of boundary value problems,

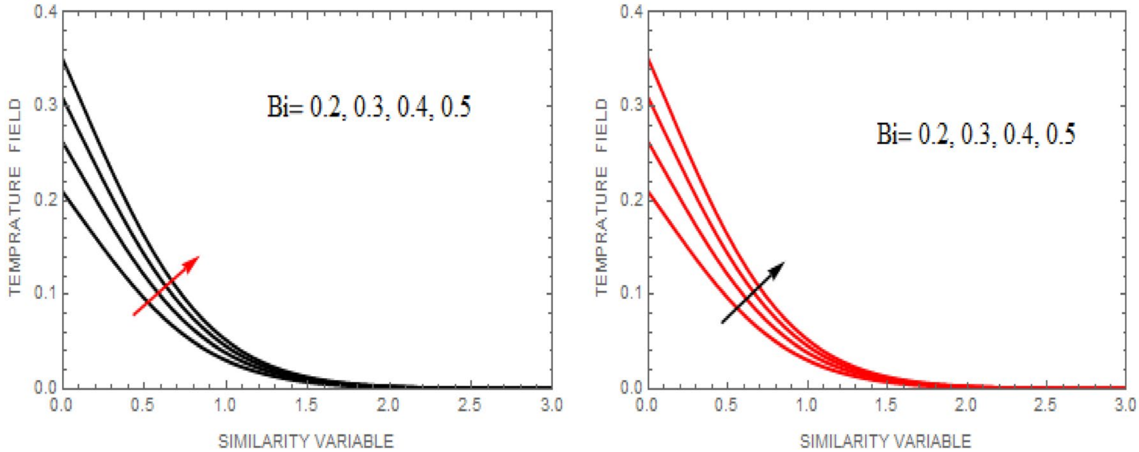

(a) Effects of Biot number Bi over $\theta(\eta)$ when $\lambda = 0$

(b) Effects of Biot number Bi over $\theta(\eta)$ when $\lambda = 0.5$

Fig. 8 Effects of Biot number Bi over $\theta(\eta)$

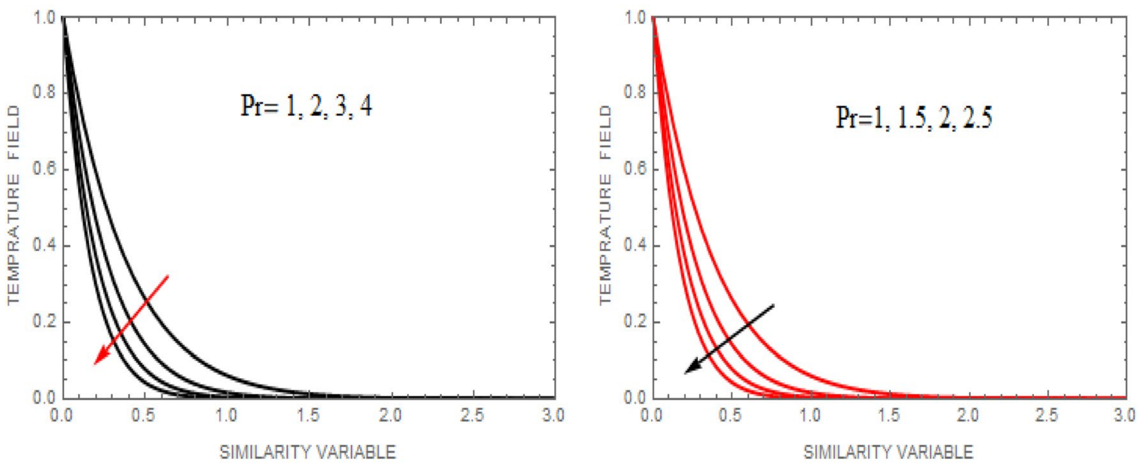

(a) Effects of Prandal number Pr over $\theta(\eta)$ when $\lambda = 0$

(b) Effects of Prandal number Pr over $\theta(\eta)$ when $\lambda = 0\ .5$

Fig. 9 Effects of Prandtl number Pr over $\theta(\eta)$

the shooting method is one of the best and most well-known schemes among all other methods. This procedure is straightforward, sensitive and free from error or complexity. First of all, convert the modeled ODEs into first-order form. Computational software Mathematica is engaged to solve these equation numerically. The steps of shooting method is given below:

Let us use f by y_1, θ by y_4, ϕ by y_6, and χ by y_8. The subsequent equations are:

$$\left.\begin{aligned}
y_1' &= y_2\\
y_2' &= y_3\\
y_3' &= \frac{1}{1-\lambda y_4}\left(y_2y_2 - y_1y_3 + My_2 - G_Ty_4 - B_ry_4 + \lambda y_5y_3\right)\\
y_4' &= y_5\\
y_5' &= -\Pr\left(y_1y_5 + Nt\left(y_5y_5\right) + Nb\left(y_5y_6\right)\right)\\
y_6' &= y_7\\
y_7' &= -\left(Ley_1y_7 + (Nt/Nb)y_5'\right) - Le\gamma y_6\\
y_8' &= y_9\\
y_9' &= Pe\left(y_8y_7 + y_7'\left(y_9+\delta\right)\right) - Sc\left(y_1y_9\right)
\end{aligned}\right| \tag{21}$$

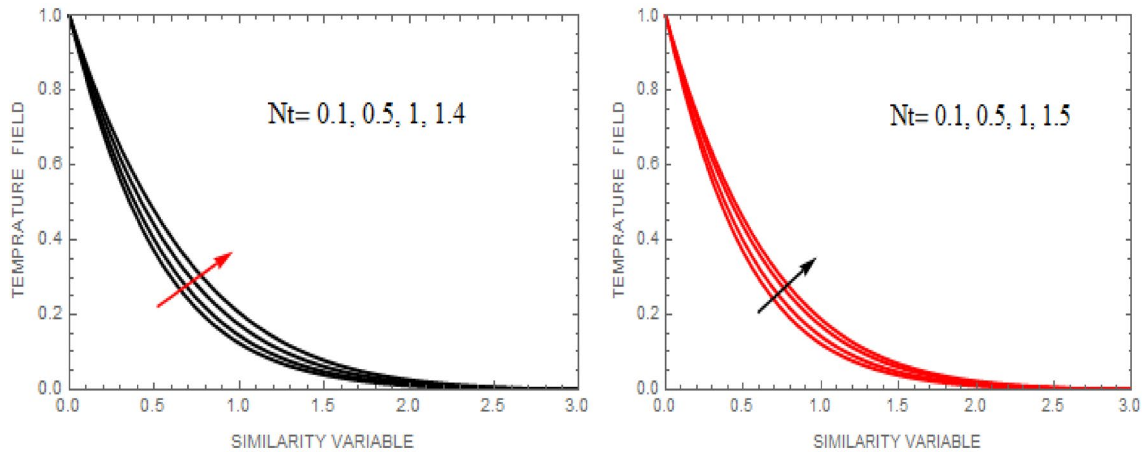

(a) Effects of thermophoresis parameter Nt over $\theta(\eta)$ when $\lambda = 0$

(b) Effects of thermophoresis parameter Nt over $\theta(\eta)$ when $\lambda = 0.5$

Fig. 10 Effects of thermophoresis parameter *Nt* over $\theta(\eta)$

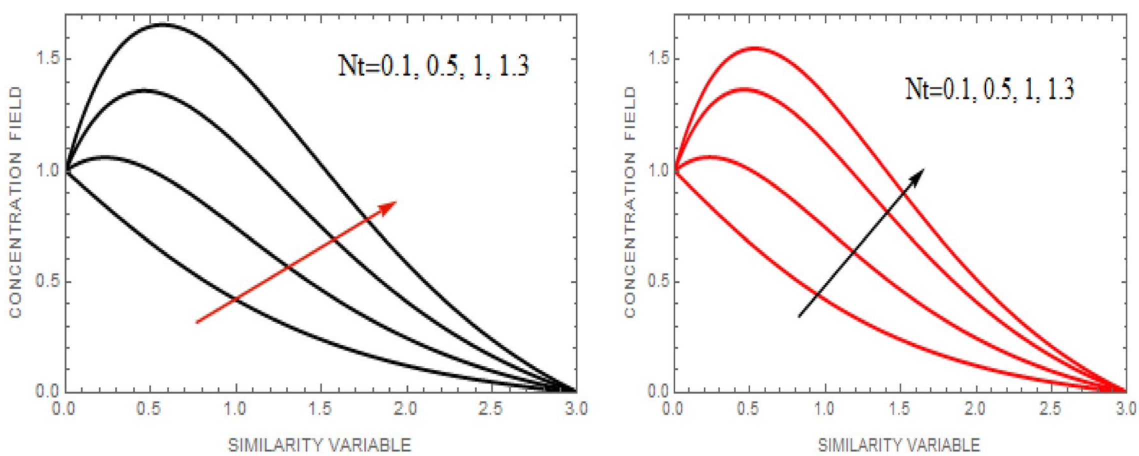

(a) Effects of thermophoresis parameter Nt over $\phi(\eta)$ when $\lambda = 0$

(b) Effects of thermophoresis parameter Nt over $\phi(\eta)$ when $\lambda = 0.5$

Fig. 11 Effects of thermophoresis parameter *Nt* over $\phi(\eta)$

Results and Discussions

This section is equipped to explore the act of non-dimensional velocity profile$f\prime(\eta)$, energy profile$\theta(\eta)$, nanofluid concentration profile $\phi(\eta)$ and density $\chi(\eta)$ under the influence of several prominent parameters like Peclet numberPe, the variable viscosityλ, Prandtl numberPr, swimming microorganism intensity variation parameterδ, thermophoresis parameterNt, bioconvection Lewis numberLb, Brownian motion parametersNb, Schmidt numberSc, concentration Grashof numberGr, thermal Grashof numbers Br, and Harman number M. Figures 3 and 4 are demonstrated to investigate the effect of Hartman number M on the velocity profile $f'(\eta)$ and temperature profile $\theta(\eta)$. Figure 2 depicts that the supplementing values of M causes retardation in the velocity profile. Temperature enhanced by increasing values of M (see Fig. 3). Hartman number includes Lorentz forces that are resistive forces. When M increased, the Lorentz force also increased, which led to a decrease in liquid flow velocity and an increase in temperature. Figure 4 shows that the increment in Gr increases the fluid speed $f'(\eta)$; it is due to occurrence of buoyancy forces. A inverse relation between Gr and $\theta(\eta)$ is obtained by Fig. 5, and an increment in values of Gr decreases the curve of$\theta(\eta)$. A straight relation between

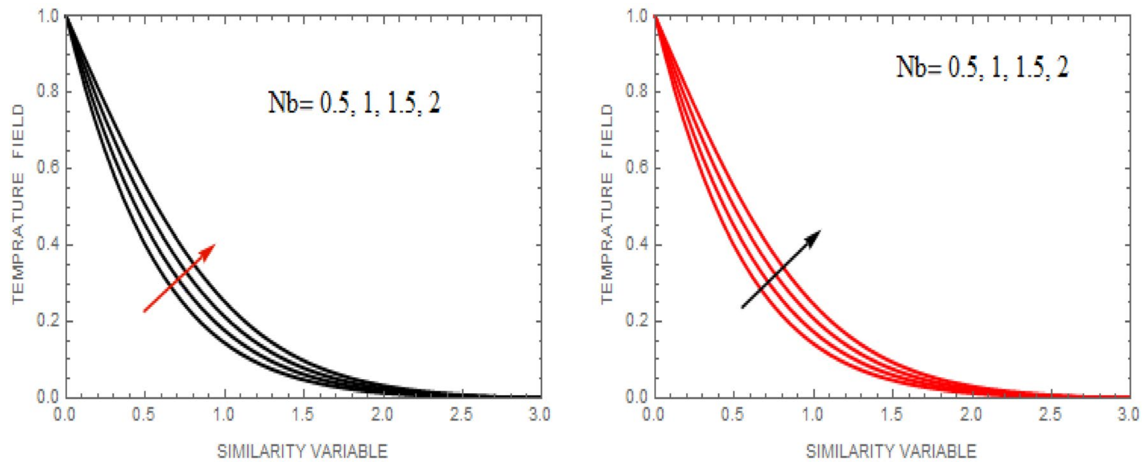

(a) Effects of brownian motion parameter Nb over $\theta(\eta)$ when $\lambda = 0$

(b) Effects of brownian motion parameter Nb over $\theta(\eta)$ when $\lambda = 0.5$

Fig. 12 Effects of *Nb* over $\phi(\eta)$

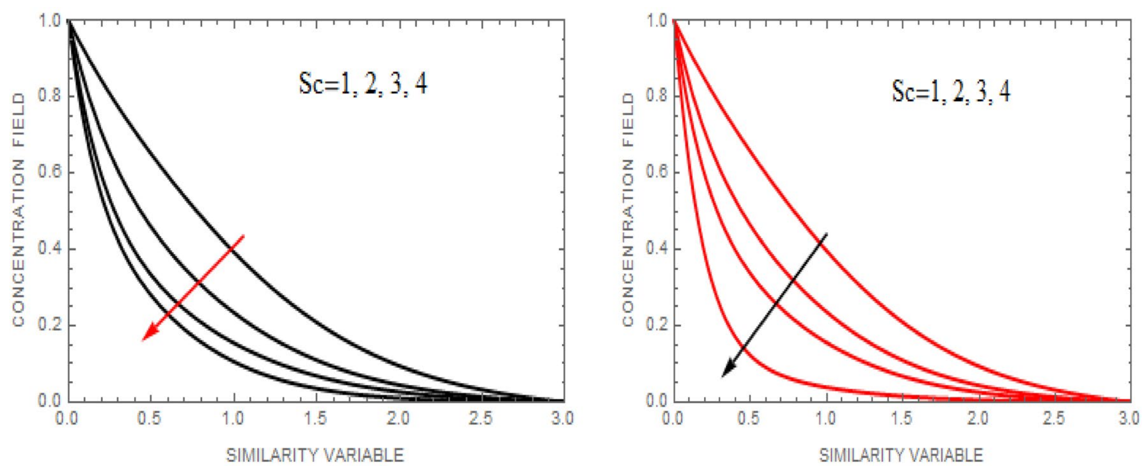

(a) Effects of Schmidt number Sc over $\phi(\eta)$ when $\lambda = 0$

(b) Effects of Schmidt number Sc over $\phi(\eta)$ when $\lambda = 0.5$

Fig. 13 Effects of Schmidt number *Sc* over $\phi(\eta)$

Br and $f'(\eta)$ is obtained by Fig. 6, and an increment in values of Br as a result increases the curve of velocity component $f'(\eta)$. Figure 7 show that the increment in Br decreases the fluid temperature$\theta(\eta)$. Figure 8 designates the distinction of Bi on fluid temperature field $\theta(\eta)$. The improvement in Biot number Bi results in much convective heat transfer and concentration rate. The dimensionless metric Biot number, which is linked to the coefficient of heat transfer, improves the temperature distribution of nanoparticles. Figure 9 shows how the Prandtl number affects the temperature field. Nanoparticle temperatures decrease as Pr is improved. Prandtl number is defined as the relationship between a fluid's thermal conductivity and thermal diffusivity. Therefore, the maximum thermal diffusivity results from the smallest Prandtl number, while the temperature and thickness of the boundary layer are reduced. Figures 10 and 11 elucidate the impact of thermophoresis parameter Nt on non-dimensional energy $\theta(\eta)$ field and volumetric concentration profile $\phi(\eta)$. These figures depicts that temperature field and volumetric concentration filed are the accumulative functions of Nt for some rising values of thermophoresis parameter. The increasing value of Nt results to raise the thermal conductivity of liquid. Tiny fluid particles are moved from a hot surface to a

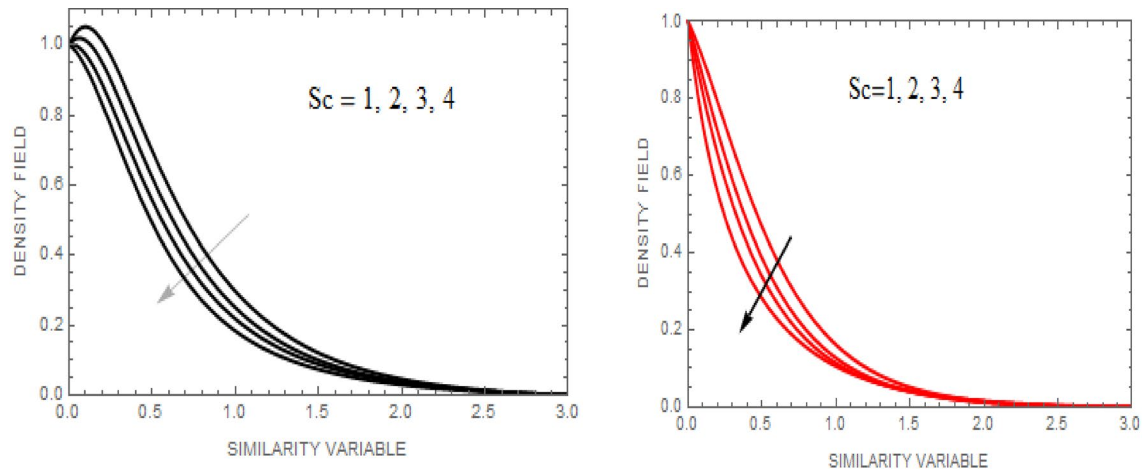

(a) Effects of Schmidt number Sc over $\chi(\eta)$ when $\lambda = 0$

(b) Effects of Schmidt number Sc over $\chi(\eta)$ when $\lambda = 0.5$

Fig. 14 Effects of Sc over $\chi(\eta)$

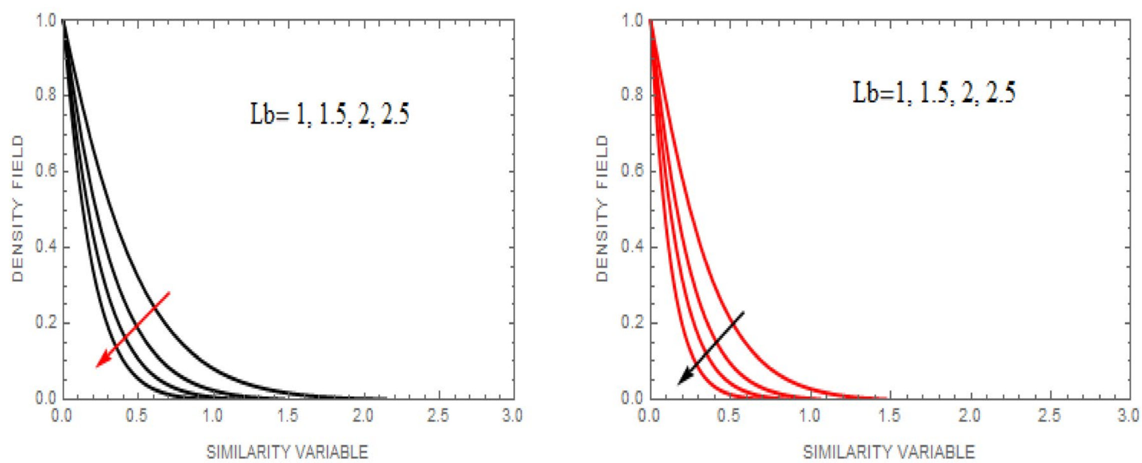

(a) Effects of bioconvection lewis number Lb over $\chi(\eta)$ when $\lambda = 0$

(b) Effects of bioconvection lewis number Lb over $\chi(\eta)$ when $\lambda = 0.5$

Fig. 15 Effects of bioconvection Lewis number Lb over $\chi(\eta)$

cool one during thermophoresis. The temperature rises as a result of the many microscopic particles leaving the hot surface, and this high temperature indicates an increase in the concentration. When a small change occurs, the concentration profile falls off and rises more quickly. The portrayal for implication of Brownian motion parameter Nb on temperature field of nanoparticles is explored in Fig. 12. By enhancing the parameter Nb energy profile improved. Usually, this Brownian parameter Nb exists because of the participation of nanoparticles. The impact of Schmidt number Sc on concentration and density profile is shown in Figs. 13 and 14. The curve of concentration distribution as well as density field is decreased as value of Sc increased. The microorganism profile under the influence of the bioconvection Lewis number is examined in Fig. 15.

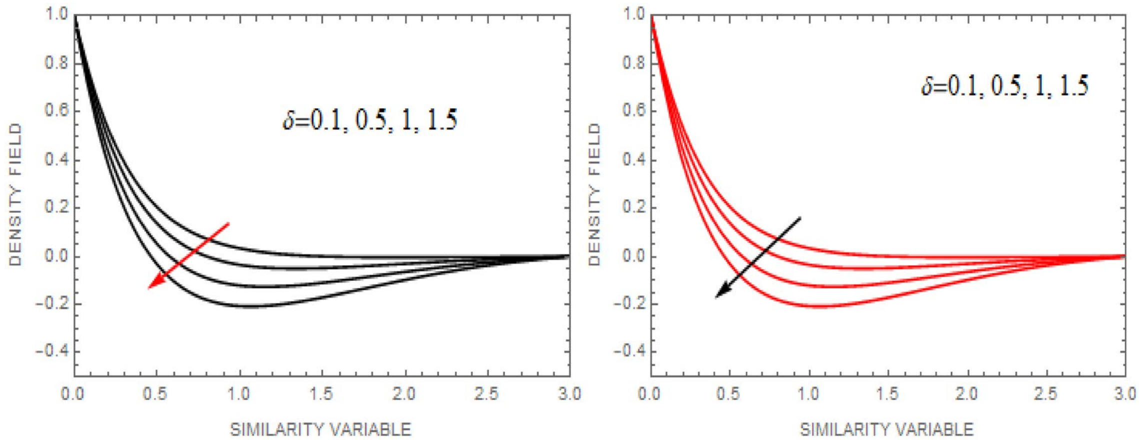

(a) Effects of swimming microorganism intensity variation parameter δ over $\chi(\eta)$ when $\lambda = 0$

(b) Effects of swimming microorganism intensity variation parameter δ over $\chi(\eta)$ when $\lambda = 0.5$

Fig. 16 Effects of swimming microorganism intensity variation parameter δ over $\chi(\eta)$

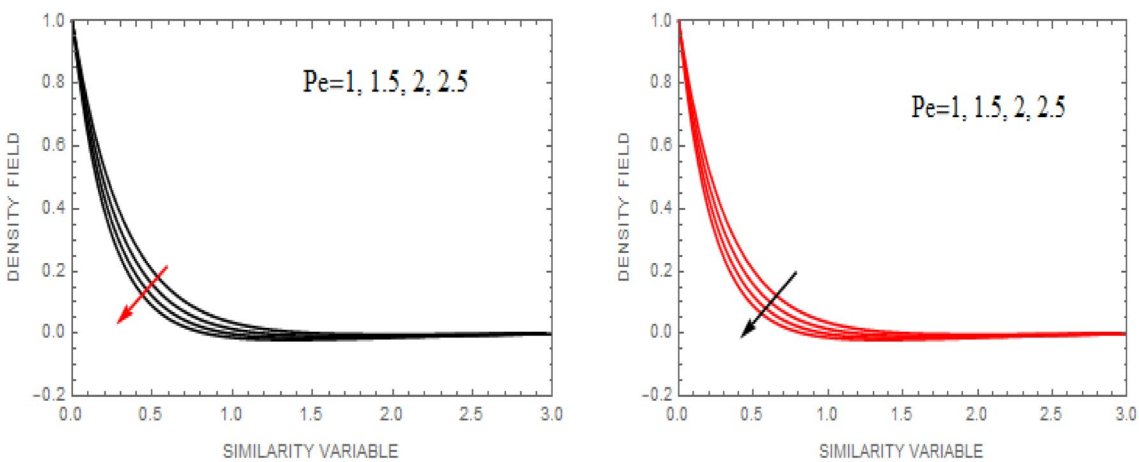

(a) Effects of Peclet number Pe over $\chi(\eta)$ when $\lambda = 0$

(b) Effects of Peclet number Pe over $\chi(\eta)$ when $\lambda = 0.5$

Fig. 17 Effects of Peclet number Pe over $\chi(\eta)$

Table 1 Comparison table for different values concentration Grashof number Br, thermal Grashof number Gr, and variable viscosity parameter λ on $-f''(0)$, $-\theta'(0)$, $-\phi'(0)$.

Br	*Gr*	lambda	$M = 0$ Bandar [27]			$M = 0$ Present		
			$-Cf$	Nu	Sh	$-Cf$	Nu	Sh
0	0.5	0	0.8826	0.08681	2.3980	0.8826	0.08681	2.3980
		0.2	0.8385	0.0864	2.3886	0.8385	0.0864	2.3886
		0.4	0.7895	0.0859	2.3664	0.7895	0.0859	2.3664
0.5	0.5	0	0.77303	0.0873	2.4144	0.77303	0.0873	2.4144
		0.2	0.73079	0.0869	2.4018	0.73079	0.0869	2.4018
		0.4	0.6839	0.0865	2.3870	0.6839	0.0865	2.3870

As the Lewis number rises, the density profile's inhibiting behavior is seen. The weak diffusivity of microorganisms is what is causing the density profile to behave slowly. Because of the strengthening that occurs as a result of the weaker diffusivity, the density profile is delayed. Figure 16 represents the effects of parameter δ called microorganism concentration difference on density profile $\chi(\eta)$. By enhancing, the values of δ density profile retarded. From Fig. 17, it is demonstrated that within the increment in bioconvection Peclet number *Pe, the* density $\chi(\eta)$ is retarded. Here, the extreme rapidity of cell swimming is enriched by increasing the value of Pe. This advanced rapidity of cell swimming is accountable in the lesser performance of $\chi(\eta)$. Comparison of current study with published work is given in Table 1.

Conclusion

Time-independent electrical magnetohydrodynamics nanofluid flow over a vertical stretching surface has been investigated. In addition, the influence of convective boundary condition along with gravitational body forces is considered. The core features of the current investigation are enumerated below:

- A decreasing act is observed in the velocity function with an increase in the value of M but enhanced by growing the value of Br and Gr.
- The temperature field improved by exaggerating the value of thermophoresis parameter Nt, biot number Bi, and Brownian motion Nb deteriorating behavior was observed in the energy distribution as boosted up in the value of Pr.
- Concentration profile is decreased for rising value of Brownian motion Nb.
- The volumetric concentration profile increased as the Brownian motion Nt value was magnified, but the Schmidt number Sc exhibited the reverse tendency.
- The density of gyrotactic motile microorganisms steadily decreases as the Peclet number Pe, Lewis number, and the value of the bioconvection increase.

Reader may read the following interested articles [33–40].

Future Recommendations

In the future, this problem may be extended in many directions, considering the following ideas:

- The impact of Joule heating.
- The impact of viscous dissipation.
- The impact of different nanoparticles.
- The impact of source and sink.

Author contribution M.J. and M.S. prepared and reviewed the manuscript. All authors are equally contributed.

Funding The authors have not disclosed any funding.

Data availability Data will be available on request.

Declarations

Conflict of interests The authors declare that they have no known competing financial interests or personal relationships that could have appeared to influence the work reported in this paper.

Ethical approval and consent to participate The research does not involve any animal trial or case studies; therefore, ethical approval is not applicable. The research does not involve any human subjects; therefore, consent to participate is not applicable.

Consent for publication All the authors provide consent for publication.

References

1. S.U. Choi, J.A. Eastman, *Enhancing thermal conductivity of fluids with nanoparticles* (No. ANL/MSD/CP-84938; CONF-951135–29). Argonne National Lab (ANL), Argonne (1995)
2. Buongiorno, J. (2006). Convective transport in nanofluids. 240–250.
3. W.A. Khan, I. Pop, Boundary-layer flow of a nanofluid past a stretching sheet. Int. J. Heat Mass Transf. **53**(11–12), 2477–2483 (2010)
4. R.K. Tiwari, M.K. Das, Heat transfer augmentation in a two-sided lid-driven differentially heated square cavity utilizing nanofluids. Int. J. Heat Mass Transf. **50**(9–10), 2002–2018 (2007)
5. N.S. Khashi'ie, N.M. Arifin, R. Nazar, E.H. Hafidzuddin, N. Wahi, I. Pop, Magnetohydrodynamics (MHD) axisymmetric flow and heat transfer of a hybrid nanofluid past a radially permeable stretching/shrinking sheet with Joule heating. Chin. J. Phys. **64**, 251–263 (2020)
6. A. Shafiq, I. Khan, G. Rasool, A.H. Seikh, E.S.M. Sherif, Significance of double stratification in stagnation point flow of third-grade fluid towards a radiative stretching cylinder. Mathematics **7**(11), 1103 (2019)
7. N. Abbas, S. Nadeem, M.Y. Malik, Theoretical study of micropolar hybrid nanofluid over Riga channel with slip conditions. Physica A **551**, 124083 (2020)
8. M.A. Mansour, A.M. Rashad, B. Mallikarjuna, A.K. Hussein, M. Aichouni, L. Kolsi, MHD mixed bioconvection in a square porous cavity filled by gyrotactic microorganisms. Int. J. Heat Technol. **37**(2), 433–445 (2019)
9. L. Kolsi, A. Abidi, M.N. Borjini, N. Daous, H. Ben Aïssia, Effect of an external magnetic field on the 3-D unsteady natural convection in a cubical enclosure. Num. Heat Transf. Part A Appl. **51**(10), 1003–1021 (2007)

10. R.K. Sharma, A. Bisht, Effect of buoyancy and suction on Sisko nanofluid over a vertical stretching sheet in a porous medium with mass flux condition. Indian J. Pure Appl. Phys. IJPAP **58**(3), 178–188 (2020)
11. L.J. Crane, Flow past a stretching plate, Zeitschrift für angewandte Mathematik und Physik. ZAMP **21**(4), 645–647 (1970)
12. M. Rezayeenik, M. Mousavi-Kamazani, S. Zinatloo-Ajabshir, CeVO4/rGO nanocomposite: facile hydrothermal synthesis, characterization, and electrochemical hydrogen storage. Appl. Phys. A **129**(1), 47 (2023)
13. M.H. Esfahani, S. Zinatloo-Ajabshir, H. Naji, C.A. Marjerrison, J.E. Greedan, M. Behzad, Structural characterization, phase analysis and electrochemical hydrogen storage studies on new pyrochlore SmRETi2O7 (RE= Dy, Ho, and Yb) microstructures. Ceram. Int. **49**(1), 253–263 (2023)
14. S. Zinatloo-Ajabshir, M.S. Morassaei, M. Salavati-Niasari, Eco-friendly synthesis of $Nd_2Sn_2O_7$–based nanostructure materials using grape juice as green fuel as photocatalyst for the degradation of erythrosine. Compos. B Eng. **167**, 643–653 (2019)
15. S. Zinatloo-Ajabshir, S.A. Heidari-Asil, M. Salavati-Niasari, Simple and eco-friendly synthesis of recoverable zinc cobalt oxide-based ceramic nanostructure as high-performance photocatalyst for enhanced photocatalytic removal of organic contamination under solar light. Sep. Purif. Technol. **267**, 118667 (2021)
16. S. Zinatloo-Ajabshir, Z. Salehi, O. Amiri, M. Salavati-Niasari, Green synthesis, characterization and investigation of the electrochemical hydrogen storage properties of $Dy_2Ce_2O_7$ nanostructures with fig extract. Int. J. Hydrogen Energy **44**(36), 20110–20120 (2019)
17. M. Jawad, M.K. Hameed, K.S. Nisar, A.H. Majeed, Darcy-Forchheimer flow of maxwell nanofluid flow over a porous stretching sheet with Arrhenius activation energy and nield boundary conditions. Case Stud. Thermal Eng. **89**, 102830 (2023)
18. M. Jawad, Insinuation of arrhenius energy and solar radiation on electrical conducting williamson nano fluids flow with swimming microorganism: completion of buongiorno's model. East Eur. J. Phys. **1**, 135–145 (2023)
19. M. Jawad, F. Mebarek-Oudina, H. Vaidya, P. Prashar, Influence of bioconvection and thermal radiation on MHD Williamson nano Casson fluid flow with the swimming of gyrotactic microorganisms due to porous stretching sheet. J. Nanofluids **11**(4), 500–509 (2022)
20. M. Jawad, M.K. Hameed, A. Majeed, K.S. Nisar, Arrhenius energy and heat transport activates effect on gyrotactic microorganism flowing in maxwell bio-nanofluid with nield boundary conditions. Case Stud. Thermal Eng. **41**, 102574 (2023)
21. M. Jawad, K. Shehzad, R. Safdar, Novel computational study on MHD flow of nanofluid flow with gyrotactic microorganism due to porous stretching sheet. Punjab Univ. J. Math. **52**(12), 5965625 (2021)
22. A. Tulu, W. Ibrahim, Effects of second-order slip flow and variable viscosity on natural convection flow of (CNTs-Fe_3O_4)/Water Hybrid nanofluids due to stretching surface. Math. Probl. Eng. **2021**, 1–18 (2021)
23. S.A. Shehzad, T. Hayat, A. Alsaedi, Influence of convective heat and mass conditions in MHD flow of nanofluid. Bull. Polish Acad. Sci. Tech. Sci. **63**(2), 465–474 (2015)
24. T. Hayat, M. Rashid, M. Imtiaz, A. Alsaedi, Magnetohydrodynamic (MHD) stretched flow of nanofluid with power-law velocity and chemical reaction. AIP Adv. **5**(11), 117121 (2015)
25. N.A. Khan, S. Aziz, N.A. Khan, Numerical simulation for the unsteady MHD flow and heat transfer of couple stress fluid over a rotating disk. PLoS ONE **9**(5), e95423 (2014)
26. T. Hayat, T. Abbas, M. Ayub, T. Muhammad, A. Alsaedi, On squeezed flow of Jeffrey nanofluid between two parallel disks. Appl. Sci. **6**(11), 346 (2016)
27. B. Bin-Mohsin, Buoyancy effects on MHD transport of Nanofluid over a stretching surface with variable viscosity. IEEE Access **7**, 75398–75406 (2019)
28. R. Safdar, M. Jawad, S. Hussain, M. Imran, A. Akgül, W. Jamshed, Thermal radiative mixed convection flow of MHD Maxwell nanofluid: implementation of Buongiorno's model. Chin. J. Phys. **77**, 1465–1478 (2022)
29. R. Safdar, I. Gulzar, M. Jawad, W. Jamshed, F. Shahzad, M.R. Eid, Buoyancy force and Arrhenius energy impacts on Buongiorno electromagnetic nanofluid flow containing gyrotactic microorganism. Proc. Inst. Mech. Eng. C J. Mech. Eng. Sci. **236**(17), 9459–9471 (2022)
30. A. Majeed, A. Zeeshan, M. Jawad, Double stratification impact on radiative MHD flow of nanofluid toward a stretchable cylinder under thermophoresis and brownian motion with multiple slip. Int. J. Modern Phys. B **23**, 2350232 (2023)
31. A. Majeed, A. Zeeshan, M. Jawad, M.S. Alhodaly, Influence of melting heat transfer and chemical reaction on the flow of non-Newtonian nanofluid with Brownian motion: Advancement in mechanical engineering. Proc. Instit. Mech. Eng. Part E J. Process Mech. Eng. **56**, 09544089221145527 (2022)
32. A.B. Disu, M.S. Dada, Reynold's model viscosity on radiative MHD flow in a porous medium between two vertical wavy walls. J. Taibah Univ. Sci. **11**(4), 548–565 (2015)
33. T. Sajid, W. Jamshed, F. Shahzad, M.R. Eid, H.M. Alshehri, M. Goodarzi, K.S. Nisar, Micropolar fluid past a convectively heated surface embedded with nth order chemical reaction and heat source/sink. Phys. Scr.. Scr. **96**(10), 104010 (2021)
34. F. Shaik, S.S.R. Al Siyabi, N. Mohammed, M. Eltayeb, Assessment of ground and surface water quality and its contamination. Int. J. Environ. Anal. Chem. **103**(6), 1449–1467 (2023)
35. M.A. Syed, Z.S. Al-Shukaili, F. Shaik, N. Mohammed, Development and characterization of algae based semi-interpenetrating polymer network composite. Arab. J. Sci. Eng. **47**(5), 5661–5669 (2022)
36. F. Shaik, Testing an aerobic fluidized biofilm process to treat intermittent flows of oil polluted wastewater. J. Eng. Res. **10**(2A), 28–38 (2022)
37. M. Jawad, A.H. Majeed, K.S. Nisar, M.B.B. Hamida, A. Alasiri, A.M. Hassan, S.W. Sharshir, Numerical simulation of chemically reacting Darcy-Forchheimer flow of Buongiorno Maxwell fluid with Arrhenius energy in the appearance of nanoparticles. Case Stud. Thermal Eng. **145**, 103413 (2023)
38. M. Jawad, K.S. Nisar, Upper-convected flow of Maxwell fluid near stagnation point through porous surface using Cattaneo-Christov heat flux model. Case Studies in Thermal Engineering **12**, 103155 (2023)
39. Jawad, M., Hussain, S., Mebarek-Oudina, F., & Shehzad, K. (2024). Insinuation of Radiative Bio-Convective MHD Flow of Casson nanofluid with Activation Energy and Swimming Microorganisms. In *Mathematical Modelling of Fluid Dynamics and Nanofluids* (CRC Press, pp. 343–362).
40. M. Jawad, M. Alam, K.S. Nisar, Investigation of thermal radiative tangent hyperbolic nanofluid flow due to stretched sheet. East Eur. J. Phys. **3**, 233–239 (2023)